environments

MDPI

Article

Sublethal Nitrite Exposure Alters Redox Status and Metabolic Functions in Adult Zebrafish

Gianluca Fasciolo [1,*,†], Eugenio Geremia [2,†], Carlos Gravato [3], Adriana Petito [1], Maria Teresa Muscari Tomajoli [2], Claudio Agnisola [1], Paola Venditti [1,*,‡] and Gaetana Napolitano [2,‡]

[1] Department of Biology, Federico II University of Naples, Complesso Universitario Monte Sant'Angelo, Via Cinthia, I-80126 Naples, Italy; adriana.petito@unina.it (A.P.); agnisola@unina.it (C.A.)
[2] International PhD Programme/UNESCO Chair "Environment, Resources and Sustainable Development", Department of Science and Technology, Parthenope University of Naples, Centro Direzionale, Isola C4, I-80143 Naples, Italy; eugenio.geremia@studenti.uniparthenope.it (E.G.); mariateresa.muscaritomajoli001@studenti.uniparthenope.it (M.T.M.T.); gaetana.napolitano@uniparthenope.it (G.N.)
[3] Departamento de Biologia Animal, Faculdade de Ciências da Universidade de Lisboa, Campo Grande, P-1749-016 Lisboa, Portugal; cagravato@ciencias.ulisboa.pt
* Correspondence: gianluca.fasciolo@unina.it (G.F.); venditti@unina.it (P.V.); Tel.: +39-081-2535080 (P.V.)
† These authors contributed equally to this work.
‡ These authors also contributed equally to this work.

Abstract

Nitrite pollution in aquatic environments, often driven by human activity, can disrupt fish physiology. Nitrite is absorbed by freshwater fish through their gills, leading to internal accumulation and interference with nitric oxide (NO) signaling, redox state, and the oxygen-carrying capacity of blood. The effects of nitrite are concentration-dependent. Although moderate environmental nitrite levels have little impact on oxygen transport, they may still interfere with NO homeostasis and cellular metabolism. We report the effects of 72 h of exposure to 10 μM nitrite on adult zebrafish blood's O_2-carrying capacity and on muscle mitochondrial activity, metabolism, and redox state. The results show that this environmentally relevant but moderate concentration of nitrite leads to decreases in fish routine oxygen consumption (rMO_2) and spontaneous activity, an increase in blood nitrosyl hemoglobin (HbNO), indicating increased NO production in the blood, accumulation of nitrite in muscle tissue, oxidative stress, and changes in muscle aerobic capacity linked to a rise in mitochondrial efficiency. Parallel to these effects, increases in antioxidant capacity, arginase activity, and urea and lactate levels were observed. Globally, these results are consistent with altered NO homeostasis in the fish body induced by nitrite stress.

Keywords: NO homeostasis; oxygen consumption; ROS; mitochondria; oxidative stress; antioxidant capacity

Academic Editor: Claude Fortin

Received: 31 October 2025
Revised: 4 January 2026
Accepted: 6 January 2026
Published: 13 January 2026

1. Introduction

Environmental pollution by nitrite (NO_2^-) is of particular concern as it is among the most biologically active and harmful compounds, due to its high reactivity and ability to interfere with essential physiological processes in aquatic organisms [1,2].

In the environment, nitrite is produced from ammonia in the presence of oxygen (O_2) by the ammonia-oxidizing bacteria. Nitrite can then be oxidized to nitrate by nitrite-oxidizing bacteria. Since ammonia-oxidizing bacteria have a higher reproductive rate than

nitrite-oxidizing bacteria, nitrite can accumulate in water bodies, often favored by human activity, resulting in highly variable concentrations [3].

In mammals, nitrite is a dynamic compound, primarily produced endogenously as an oxidative metabolite of nitric oxide (NO), a short-lived, rapidly diffusing signaling molecule present in most organisms [4]. Nitrite serves as a storage pool and a source of NO under hypoxic and stressful conditions [4–9], and it also regulates protein function and gene expression [5,10,11]. Under normal physiological conditions, nitrite levels are kept low (0.05–0.5 μM), and turnover is rapid, with half-lives estimated in minutes to hours [12]. Continuous production via rapid oxidation of NO is balanced by further oxidation to nitrate or reduction back to NO by various proteins (the non-canonical pathways for NO synthesis [6]), while only a minor amount originates from nitrate reduction in food [7].

Nitrite plays a similar role in NO homeostasis in fish as in mammals, particularly under hypoxic conditions, which are common in aquatic environments [13–15]. As in mammals, under hypoxic conditions, when nitric oxide synthase (NOS) activity is constrained by insufficient oxygen for nitric oxide (NO) synthesis, nitrite is reduced to NO by various proteins, particularly deoxymyoglobin, myoglobin, and globin X [16–18]. This process induces vasodilation and increases tissue perfusion [19,20]. The evolutionary significance of this role of nitrite is supported by the finding that nitrite-reducing capacity is higher in hypoxia-tolerant species [16,17,19,21].

In fish, the primary endogenous source of nitrite is the oxidation of NO, as in mammals. However, freshwater fish also have a putatively significant exogenous source of nitrite. They can absorb nitrite from the environment via the gills, thereby contributing to the internal nitrite/NO pool. Nitrite enters fish through gill cells involved in chloride and bicarbonate exchange via the same transporter used for chloride ions, acting as a competitive inhibitor of chloride uptake [22–25]. Fish can accumulate nitrite in their blood and tissues to levels up to 60 times higher than the environmental concentration [22,25,26]. This accumulation is time-dependent and can vary with species, water chemistry, and exposure duration [24,26].

Unpolluted freshwater environments contain very low nitrite concentration, usually below 1 μM [27–29], due to rapid bacterial nitrification [27]. At these environmental concentrations, nitrite typically has little effect on the physiology of aquatic animals [3]. However, anthropogenic pollution from nitrogen-based compounds, released through agricultural runoff, industrial discharges, and urban wastewater, may induce nitrite accumulation to levels exceeding 400 μM [30]. In nitrite-rich environments, nitrite accumulation in the fish body can cause a wide array of physiological disturbances. In particular, it can disrupt oxygen transport by converting hemoglobin to non-functional methemoglobin (metHb), inducing significant tissue hypoxemia [23], and altering NO formation rate, bioactivity, and scavenging, disrupting NO-dependent signaling [4,24,26,31].

NO homeostasis is a very complex process, and any alteration in the nitrite turnover may affect the numerous NO-dependent biochemical pathways as well as the rate of peroxynitrite ($ONOO^-$, a potent oxidant that can significantly contribute to oxidative stress) formation and its consequences on the cellular redox state (see Figure 1 in reference [4]). Moreover, nitrite stress may also affect the arginine homeostasis and the competition for substrate between NOS and arginase [32]. The interplay between nitrite stress, redox homeostasis, and mitochondrial function is particularly critical in muscle tissue [5,33]. Particularly significant is the NO capacity to bind mitochondrial cytochrome oxidase (COX and modulate respiratory function [34]. Mitochondria, as the primary sites of aerobic respiration, are highly sensitive to changes in oxygen availability and redox conditions [35]. Alterations in mitochondrial efficiency or an increase in reactive oxygen species (ROS) production can disrupt energy metabolism, leading to lipid peroxidation and triggering cell death pathways [35]. NO is a potent and reversible inhibitor of COX, and mitochondria can

finely regulate the levels of O_2 in their surroundings via NO production from nitrite [36]. Moreover, alterations in NO homeostasis, especially when combined with reduced mitochondrial efficiency or increased superoxide formation, will lead to the formation of $ONOO^-$ [37]. Several studies have demonstrated that millimolar nitrite concentrations affect redox homeostasis and modulate metabolic activity in various fish species [23,38,39].

Research on acute exposure of fish to environmental nitrite typically involves testing at relatively high concentrations, up to 6 mM [32,39–42]. At these concentrations, the nitrite effects are likely dominated by metHb-dependent hypoxemia, with consequent severe tissue hypoxia [23]. Conversely, micromolar concentrations of environmental nitrite may induce effects independent of nitrite-induced hypoxemia, offering insights into the direct consequences of altered nitrite turnover in the animal on NO homeostasis, mitochondrial function, and redox state. Here, we examined the effects of a moderate, sub-lethal nitrite concentration (10 micromolar) exposure on zebrafish (*Danio rerio*), a well-established model to study the physiology of freshwater fish [43]. Specifically, the study examined changes in the percentages of blood's oxyhemoglobin (HbO_2), metHb, and nitrosyl hemoglobin (HbNO, an index of NO level in the blood) [44,45], as well as the effects on mitochondrial respiratory chain activity (ETC), oxidative metabolism, ROS content, lipid peroxidation levels, antioxidant defense responses, arginase activity, and urea content in muscle. We also analyzed mitochondrial content and dynamics by assessing the protein content of cytochrome c, mitofusin, and dynamin.

2. Materials and Methods

2.1. Animals

Wild-type zebrafish (230 juveniles of both sexes; body length < 1.5 cm; mean body weight approximately 0.5 g) were obtained from the fish facility of the Department of Biology, University of Naples Federico II. The fish were maintained at 27 °C in dechlorinated water fully aerated (dissolved oxygen > 8 mg/L, measured with a YSI 5357 Micro Probe, YSI, Yellow Springs, Ohio, USA), continuously filtered and aerated under a 10:14 h light–dark photoperiod before experimentation. Water quality was assessed daily to measure nitrate, nitrite, general hardness (GH), alkalinity (KH), and pH using a commercial water-quality test kit (JBL GmbH & Co. KG, Dieselstraße 3, 67141 Neuhofen, Germany). Water pH was between 7.2 and 7.4, nitrate and nitrite levels were 0 mg/L, water hardness ranged from 6 to 8 °dGH, and alkalinity ranged from 4 to 6 °dKH. Chloride, as assessed by the method of Belcher et al. [46], was lower than 100 µM.

Fish were fed daily with commercial pelleted food (Tetramin; Tetra, Melle, Germany) containing 47% crude protein, 6% moisture, and an energy content of 20.1 kJ/g dry weight. Twice a week, Tetramin was replaced with *Chironomus* larvae (Eschematteo s.r.l., Parma, Italy; 7.01% crude protein, 89% moisture, 21.9 kJ/g dry weight).

Animal care and experimental procedures were conducted in accordance with European and Italian laws (2010/63 and 26/2014, respectively) and approved by the University of Naples Federico II Committee for the Ethics of Animal Experiments and the Italian Minister of Health (N. 767/2023-PR, 30 August 2023).

2.2. Treatment and Experimental Protocols

Zebrafish were randomly assigned to one of two groups: a control group (C group, N = 115) exposed for 72 h to water identical to the maintenance water (C-water), and a nitrite group (NO_2 group, N = 109) exposed for 72 h to 10 µM sodium nitrite ($NaNO_2$) added to the maintenance water (NO_2-water). One-third of the water was replaced every 24 h intervals. Water quality was assessed daily for the maintenance water. Nitrate levels remained undetectable. Nitrite level was checked daily using the Griess method [47].

For both the C and NO_2 groups, three independent experimental procedures were utilized, as described below. Animals were distributed into 3 L tanks to enable tank replication and test the effect of the tank on the evaluated parameters (see Supplementary Materials, Experimental design for further details). Each tank housed between 3, 4, or 10 fish, depending on the planned measurements. Each tank contained a water volume adjusted to achieve a fish density of 5 individuals per liter, in line with the European Commission Guidelines for the treatment of animals used for scientific purposes (2024) [48]. At the end of the exposure period, fish were euthanized with benzocaine (0.1 mg/mL).

2.2.1. In Vivo Measurements and Blood Analysis

Eight animals were randomly distributed between two tanks: 4 in C-water and 4 in NO_2-water. This treatment was replicated 4 times (N = 4), for a total of 32 animals. At the end of the exposure period, some randomly selected animals were used to measure routine oxygen consumption (rMO_2) and spontaneous activity individually. After completing these measurements and allowing recovery, blood samples were collected to determine the percentages of oxyhemoglobin (HbO_2), methemoglobin (metHb), and nitrosyl hemoglobin (HbNO). Blood from different individuals was also sampled to determine the blood's nitrite content.

2.2.2. Muscle Tissue Analysis

Sixty animals were randomly assigned to six pairs of tanks, with three pairs containing C-water and three containing NO_2-water. Following the exposure period, animals from each pair were used to prepare three distinct types of tissue homogenates for the assessment of (1) nitrite content, (2) urea levels, lactate concentration, and arginase activity, and (3) oxidative metabolism. This procedure was replicated 3 times (N = 3), yielding a total of 180 animals. Protein concentrations in all homogenates were measured using the Bio-Rad Bradford colorimetric assay and a commercial kit (Bio-Rad, Hercules, CA, USA). All animal and experimental data were included in the analysis.

2.2.3. Western Blot Analysis

Six animals were randomly distributed between two tanks, one containing C-water and the other NO2-water. At the end of the exposure period, animals from each tank were used to prepare muscle homogenate for Western blot analysis of cytochrome c, dynamin, and mitofusin. The procedure was repeated 3 times (N = 3), for a total of 18 animals.

2.3. Routine Oxygen Consumption (rMO_2) and Spontaneous Activity

Routine metabolism (rMO_2) is the oxygen consumption of fish at rest and in a fasted state, but with spontaneous basal activity [49], so it requires simultaneous measurement of oxygen consumption and animal activity. The rMO_2 was measured at 27 °C using a closed respirometry system [49] consisting of a thermostatic plexiglass chamber (125 mL) equipped with an oxygen microelectrode (YSI 5357 Micro Probe, Yellow Springs, OH, USA) that continuously monitored the oxygen content in the water. The microelectrode was connected to an Oxygen Monitoring System (YSI 5300 A, Yellow Springs, OH, USA), and the data output was captured by an analogical-to-digital interface (Pico Technology Ltd. St. Neots PE19 8YP, UK) connected to a PC with Picolog software version 5.25.3. for automated data acquisition. The water in the respirometer was fully aerated and continuously stirred to ensure uniform oxygen distribution. The selected fish from each group (n = 10) were individually transferred into the respiratory chamber. After an adaptation period, the chamber was sealed, and the decrease in PO_2 was recorded. The decline in PO_2 was not allowed to exceed 15%. Oxygen consumption rates were determined from the linear

decrease in water oxygen concentration, with rates calculated using linear regression analysis. Fish rMO_2 values were reported as mg O_2 per hour per gram of body weight.

Spontaneous activity of each fish was assessed by counting the number of turns per minute while in the respiratory chamber [50]. Measurements were obtained by analyzing video recordings taken during oxygen consumption assessments.

2.4. Blood Sample Collection, Hemoglobin Spectral Deconvolution, and Blood Nitrite Content Determination

Given the capacity of nitrite to compete with oxygen for hemoglobin [23], we assessed the blood content of HbO_2, MetHb, and HbNO. Blood samples were collected from each zebrafish (n = 10 for both the control and the NO_2^- groups) after anesthesia with benzocaine at a concentration of 0.1 mg/mL. Using heparinized glass Pasteur pipettes (tip diameter: 0.8–0.9 mm), blood was collected by capillarity after a lateral incision at the level of the anus to reach the caudal vein. The volume of the collected blood was calculated from the height of the blood column inside the capillary and the capillary's inner diameter. Typically, between 4 and 10 µL of blood was obtained from each fish. The collected blood samples were transferred into pre-calibrated microtubes containing 1 mL of 20 mM phosphate buffer (pH 7.3). To remove cellular debris, the samples were centrifuged for 2 min at 12,000× *g*. After centrifugation, 1 mL of the supernatant was immediately transferred into cuvettes for hemoglobin spectrum scan, using a Beckman Coulter (Brea, CA, USA) DU 800 spectrophotometer in the range of 480–700 nm with 0.2 nm increments. The scan was completed within 3 min of blood sample preparation. The spectra were successively analyzed with the deconvolution technique [51]. Assuming that the hemoglobin sample is a mixture of HbO_2, deoxyhemoglobin, metHb, and HbNO, and according to the Lambert-Beer law, the absorbance (A) at each wavelength (λ) will be the sum of the contributions of each of the four forms of Hb, according to the equation:

$$A_\lambda = \left[\left(C_{oxyHb} \times \epsilon_{oxyHb}\right) + \left(C_{deoxyHb} \times \varepsilon_{deoxyHb}\right) + \left(C_{metHb} \times \epsilon_{metHb}\right) + \left(C_{HbNO} \times \varepsilon_{HbNO}\right)\right] \times l \quad (1)$$

C is the millimolar concentration of each Hb form, ε represents the molar extinction coefficient of each Hb form at wavelength λ, and l represents the thickness of the cuvette (1 cm). The relationship between ε and λ for each Hb form, in the range 480–700 nm, was previously determined as described by Jensen [51].

Spectral analysis for deconvolution was performed by fitting Equation (1) to the sample spectrum using nonlinear regression (least squares) based on the Levenberg–Marquardt algorithm, with Origin 7 statistical software (OriginLab Corporation, Northampton, MA, USA).

Blood samples were also collected from 6 additional individuals from each group as above and transferred to a solution containing 4.31% $ZnSO_4 \bullet 7H_2O$ and 1.45% NaOH for protein precipitation [26], followed by centrifugation and determination of nitrite using the Griess method [47] with the Griess reagent from Sigma-Aldrich. Absorbance was measured at 520 nm using a multimode microplate reader (Synergy™ HTX Multimode Microplate Reader, BioTek, Santa Clara, CA, USA). Blood nitrite was expressed as micromoles per liter.

2.5. Muscle Nitrite, Lactate, and Urea Content, and Arginase Activity

For nitrite levels determination, muscles were homogenized in a solution containing 2.35% $ZnSO_4 \bullet 7H_2O$ and 1.45% NaOH [26], incubated for 1 h on ice, and then centrifuged at 20,000× *g* for 15 min at 4 °C. Nitrite determination was performed using the Griess method, as described above. Nitrite levels were expressed as nmol of nitrite per gram of tissue.

Since nitrite stress can affect NO homeostasis by arginase stimulation and urea accumulation [32], we evaluated urea content and arginase activity in the muscle of zebrafish.

To evaluate urea and lactate levels, aliquots of muscle samples were treated according to Dunn and Hochachka [52]. Briefly, the muscles were homogenized for 1 min (20% w/v) in 7% perchloric acid using a glass Potter at 500 rpm. Homogenates were centrifuged at 20,000× g for 15 min at 4 °C. The supernatants were neutralized at pH 7.5 with 3 M K_2CO_3 and 0.1 M triethanolamine, and then centrifuged at 20,000× g for 15 min at 4 °C. The urea content in muscle homogenates was measured using the diacetyl-monoxime procedure [53]. In brief, 1 mL of homogenate was added to 0.5 mL of urea reactant (8.3 mg/mL of 2,3-Butanedion monoxime, 0.2 mg/mL thiosemicarbazide, and 0.1 mg/mL $FeCl_3$ in 32% H_2SO_4), then the mixture was heated (100 °C) for 10 min in the dark. After cooling, urea levels were detected spectrophotometrically at 535 nm using a multimode microplate reader (Synergy™ HTX Multimode Microplate Reader, BioTek). Urea content was expressed as µmol of urea per g of tissue.

The same homogenates were used to determine the arginase activity as the rate of urea formation, as described by Romero et al. [54]. Briefly, aliquots of homogenates were treated for one hour with $MnSO_4$ (100 mM, pH 7.0 at 27 °C) to activate the enzyme. Then, L-Arginine (285 mM, pH 9.5) was added, and the mixture was incubated for 30 min at 27 °C. Urea levels were measured as previously described. Arginase activity was expressed as µmol of urea produced per hour per g of tissue.

Lactate concentrations in muscle homogenates were quantified in aliquots containing 0.015 mg of protein using a spectrophotometric enzymatic assay adapted from Rees et al. [55]. In this assay, L-lactate is oxidized to pyruvate by L-lactate dehydrogenase (5000 U/mL) in the presence of NAD^+ (25 mM). The reaction was carried out in a glycine–hydrazine buffer (0.5 M glycine, 0.4 M hydrazine sulfate, pH 9.5), which facilitates hydrazone formation and drives the reaction to completion. The concentration of lactic acid in the sample, which is stoichiometrically correlated to the amount of NADH formed in the enzymatic reaction, was determined at 340 nm using a multimode microplate reader (Synergy™ HTX Multimode Microplate Reader, BioTek). The lactate concentration was expressed as micromoles of lactate per gram of tissue.

2.6. Tissue Aerobic Capacity Evaluation

The effects of nitrite on the aerobic metabolic capacity of muscle were studied by measuring oxygen consumption in both homogenates and isolated mitochondria. We evaluated the coupled mitochondrial respiration and cytochrome c oxidase activity (an index of maximal aerobic capacity, [56]) in Lubrol-treated homogenates, as well as the oxygen consumption in frozen, uncoupled mitochondria, to gain insight into the function of the electron transport chain complexes.

Muscle samples were homogenized 1:5 in ice-cold homogenization medium (HM) (220 mM mannitol, 70 mM sucrose, 1 mM EDTA, 10 mM Tris, pH 7.4) using a glass Potter-Elvehjem homogenizer set at a standard speed (500 rpm) for 1 min. The homogenate was divided into three aliquots. One was rapidly frozen in liquid nitrogen for later determination of COX activity and redox parameters. A second aliquot was used to determine the homogenate respiration rate immediately. Finally, the third aliquot was used to isolate mitochondria by differential centrifugation. Briefly, the homogenate was first cleared of cellular debris and nuclei by centrifugation at 500 g for 10 min at 4 °C. The resulting supernatant was then centrifuged at 9000× g for 10 min to pellet mitochondria. The mitochondrial pellet was resuspended in wash buffer (WB) (220 mM mannitol, 70 mM sucrose, 1 mM EGTA, 20 mM Tris, pH 7.4) and centrifuged at 9000× g for 10 min. This washing step was repeated twice, after which the mitochondrial pellet was resuspended in WB. Total mitochondrial protein was calculated using the Bradford colorimetric protein assay of the Bio-Rad Bradford (Bio-Rad, Hercules, CA, USA). An aliquot of isolated mitochondrial preparation was

used within 1 h of isolation to measure mitochondrial oxygen consumption, while the rest was frozen for later determination of COX and electron transport chain (ETC) activity in uncoupled mitochondria.

Oxygen consumption in both homogenates and isolated mitochondria was measured at 27 °C using a Hansatech respirometer. Measurements were conducted in 1.0 mL of incubation medium (145 mM KCl, 30 mM Hepes, 5 mM KH_2PO_4, 3 mM $MgCl_2$, 0.1 mM EGTA, 0.1% BSA, pH 7.4) containing either 0.01 g of tissue or 0.2 mg of mitochondrial proteins. Oxygen consumption was determined under two conditions: in the presence of 500 µM ADP (State 3) and in its absence (State 2). Pyruvate plus malate (10/2.5 mM) served as substrates. The results were expressed as nmol O per minute per g of tissue or per mg of protein.

Complex IV (cytochrome c oxidase, COX) activity in both homogenates and isolated mitochondria was determined using a polarographic method [57]. Measurements were carried out in a 1.0 mL buffer solution containing 30 µM cytochrome c, 10 mM sodium malonate, 75 mM HEPES, 4 µM rotenone, and 0.5 mM 2,4-dinitrophenol, pH 7.4. An aliquot of muscle homogenate or mitochondrial suspension (containing 0.01 g tissue or 0.2 mg of protein, respectively), solubilized with 1% Lubrol, was added to this buffer along with a mixture of TMPD and ascorbate (30 mM and 400 mM, respectively). COX activity was expressed as µmol O consumed per minute per g of tissue or mg of protein.

The assessment of the activity of the electron transport chain (ETC) segments between complexes I and IV was performed following the method described by Acin-Perez et al. [58]. Briefly, oxygen consumption was determined at 27 °C on uncoupled mitochondria using a Hansatech respirometer in 1.0 mL of incubation medium (145 mM KCl, 30 mM Hepes, 5 mM KH_2PO_4, 3 mM $MgCl_2$, 0.1 mM EGTA, 20 µM cytochrome c, 0.1% BSA, pH 7.4). The procedure used 0.2 mg of mitochondrial proteins. The assay was performed by sequentially adding the following reagents: 1 mM NADH (to evaluate the activity of the ETC from complexes I to IV); 2 µM rotenone (ROT, to inhibit electron transport from complex I); 5 mM succinate (to assess the activity from complex II to IV); 4 µM antimycin A (AA, to block electron transport at complex III); 0.5 mM TMPD and 1 mM ascorbic acid (to evaluate the activity of complex IV). ETC activity was expressed as nmol oxygen per minute per mg of mitochondrial protein.

2.7. Western Blot Analysis of Cytochrome c, Dynamin, and Mitofusin

Mitochondrial population dynamic was evaluated by determining, by Western blot, the levels of cytochrome c, as an index of the mitochondrial population content, and those of dynamin and mitofusin, indices of mitochondrial fusion and fission processes, respectively [57,59].

Immunoblotting was performed as previously reported [60]. For each biological replicate (N = 3) the trunk skeletal muscle from an individual fish was collected and homogenized in 300 µL of RIPA buffer (150 mM NaCl, 1.0% Triton X-100, 0.5% sodium deoxycholate, 0.1% SDS, 50 mM Tris, pH 8.0), to which antiprotease cocktail (Merck, Life Science S.r.l., Milano, Italy) was added. After 15 min of incubation, the lysates were centrifuged at 12,000× *g* for 10 min at 4 °C.

Protein content of each supernatant was quantified using a Bradford colorimetric commercial kit (Bio-Rad, Hercules, CA, USA). 40–80 µg of protein lysate was separated in an SDS-PAGE gel and transferred to a PVDF membrane. The blots were blocked with a blocking solution (5% bovine serum albumin) for 1.5 h at room temperature. The blots were then incubated with the following commercially available primary antibodies: cytochrome c (1: 1000, SC-7159, Santa Cruz, San Diego, CA, USA); Dynamin-related protein 1 (DRP1)

(1:1000, sc-271583, Santa Cruz, San Diego, CA, USA), Mitofusin-1 (MFN1) (1:1000, sc-166644, Santa Cruz, San Diego, CA, USA).

As housekeeping proteins, beta-actin (β-actin) (1:1000, sc-47778, Santa Cruz, San Diego, CA, USA) was used. Secondary antibodies were purchased from Santa Cruz (1:5000, anti-rabbit sc-2030, anti-mouse sc-525409, Santa Cruz, San Diego, CA, USA). After overnight incubation with the primary antibodies at 4 °C, the blots were washed and subsequently incubated with the appropriate secondary antibody for 1 h. Protein bands were visualized using a chemiluminescent detection kit (ElabScience; Microtech, Naples, Italy) according to the manufacturer's instructions. Quantitative analysis of band intensity was carried out on ChemiDoc-acquired images.

2.8. Redox Homeostasis Evaluation (ROS Content, Lipid Oxidative Damage, Susceptibility to Oxidants, and Total Antioxidant Capacity)

Since nitrite-induced metabolic alterations can be associated with changes in redox homeostasis, we evaluated ROS levels, lipid oxidative damage (hydroperoxides, Hp), susceptibility in vitro to oxidants (ΔHp), and total antioxidant capacity (TAC).

ROS levels in muscle homogenates and isolated mitochondria were assessed by monitoring the ROS-dependent oxidation of 2′,7′-dichlorodihydrofluorescin diacetate (DCFH-DA), a nonfluorescent probe, to the fluorescent product dichlorofluorescein (DCF) as described by Napolitano et al. [57]. Fluorescence was detected using a multimode microplate reader (Synergy™ HTX, BioTek) set to excitation and emission wavelengths of 485 and 530 nm, respectively. Background signal, resulting from the DCFH auto-oxidation in the absence of biological samples, was subtracted using parallel blanks. ROS levels were expressed as relative fluorescence unit (RFU) per mg of protein.

Lipid peroxidation in tissue homogenates was assessed by quantifying Hp levels in samples diluted in 0.1 M monobasic phosphate buffer, pH 7.4 [61]. The decrease in NADPH absorbance, resulting from the coupled reactions of glutathione peroxidase and glutathione reductase in the presence of GSH, was monitored at 340 nm. All measurements were performed using a multimode microplate reader (Synergy™ HTX, BioTek). Hp values were expressed as nmol of NADPH consumed per minute per gram of tissue.

The ΔHp of muscle homogenates was assessed by the changes in hydroperoxide levels due to the treatment of 10% tissue homogenate with iron and ascorbate (Fe/As), at a concentration of 100/1000 μM, for 10 min at room temperature. The reaction was blocked by adding 0.2% 2,6-di-tert-butyl-p-cresol (BHT), and the hydroperoxide levels were evaluated as previously described.

TAC of the tissue homogenate was assessed using a decolorization assay [62] based on the radical monocation of 2,2′-azinobis- (3-ethylbenzothiazoline-6-sulfonic acid) ($ABTS^{\bullet+}$). The $ABTS^{\bullet+}$ was generated by oxidizing ABTS (7 mM) with potassium persulfate (245 mM). The resulting radical is subsequently decolorized by the antioxidants present in the muscle homogenates, in proportion to their concentration and antioxidant strength. A 2.5 mM stock solution of 3,5-Di-tert-4-butylhydroxytoluene (BHT) was used to construct a calibration curve. $ABTS^{\bullet+}$ decolorization was measured with a multimode microplate reader (Synergy™ HTX, BioTek) at 740 nm. TAC values were expressed as mmol BHT equivalents per mg of protein.

2.9. Statistical Analysis

GraphPad Prism, version 9.0 (GraphPad Software, Inc., San Diego, CA, USA). The effect of tank replicates (tank-treatment interaction) was tested by a Two-way ANOVA (mixed Model) and was never found significant (see Supplementary Materials). The Shapiro–Wilk test and the F-test were used to assess normality and equal variance, respectively. The effect or treatment was tested by applying the unpaired T-test, with the Welch's correction in case

of inequality of variances. *p*-values of * $p < 0.05$, ** $p < 0.01$, *** $p < 0.001$, and **** $p < 0.0001$ were used to indicate statistical significance between the two experimental groups.

3. Results

3.1. Effect of Nitrite Exposure on the Oxygen-Carrying Capacity of Blood, Spontaneous Activity and rMO_2, and on Blood and Tissue Nitrite Levels

The oxyhemoglobin (HbO_2) content of fully oxygenated blood, expressed as a percentage of total hemoglobin, showed a significant 2% decrease in zebrafish exposed to 10 µM nitrite compared with the control group (Figure 1A), slightly reducing the oxygen-carrying capacity of blood. Notably, this reduction was accompanied by the significantly corresponding increase in the nitrosyl hemoglobin (HbNO) (Figure 1C), while the methemoglobin (MetHb) content remained unchanged (Figure 1B).

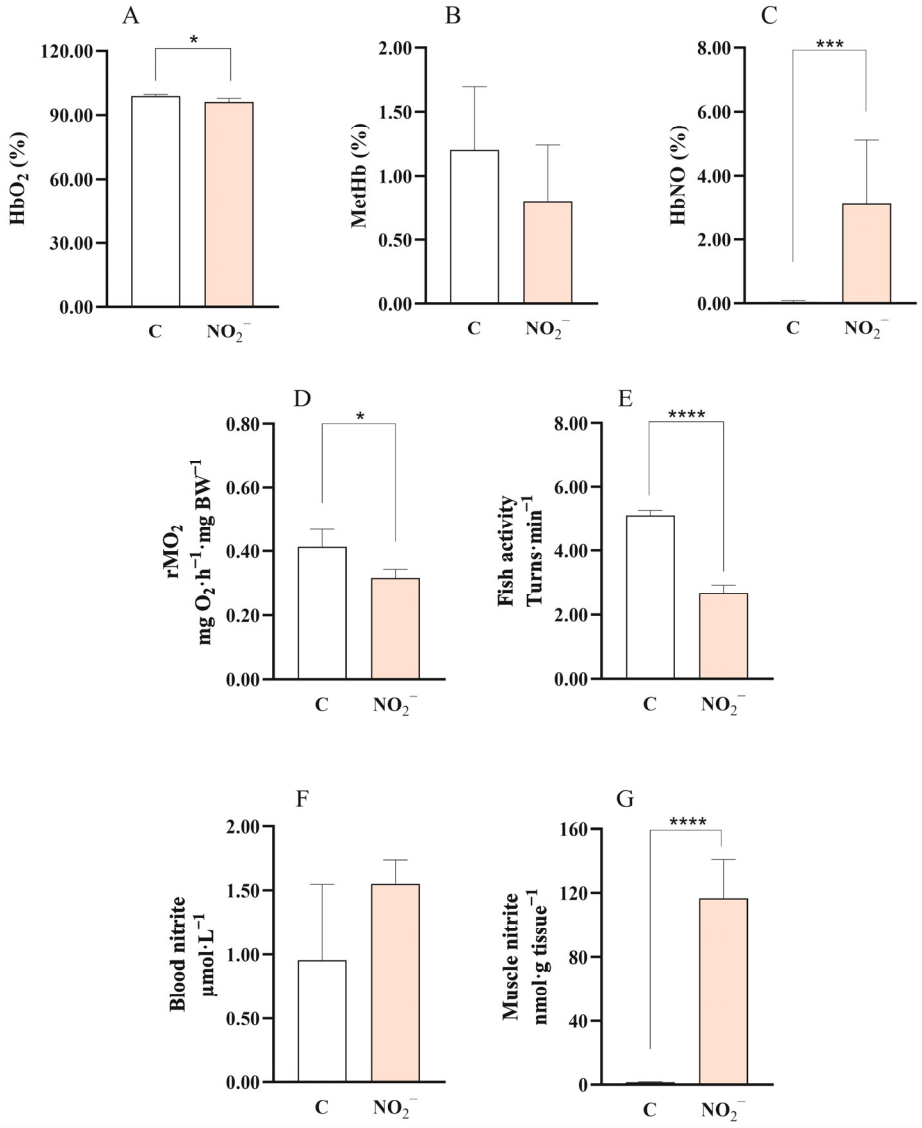

Figure 1. Top row: Blood levels of HbO_2 (**A**), MetHb (**B**), and HbNO (**C**), expressed as percentages of total hemoglobin in the plasma of control and 10 µM nitrite-exposed zebrafish. Middle row: Routine oxygen consumption (rMO_2) (**D**) and spontaneous activity (number of turns per minute) (**E**) in control and 10 µM nitrite-exposed zebrafish. Bottom row: Nitrite concentrations in blood (**F**) and muscle tissue (**G**) of control and 10 µM nitrite-exposed zebrafish. Data in panels (**A**–**E**) represent mean ± SEM of 4 replicated experiments; data in panels (**F**,**G**) represent mean ± SD of 4 replicated experiments. * $p < 0.05$; *** $p < 0.001$; **** $p < 0.0001$.

Both routine oxygen consumption (rMO_2) and spontaneous activity of zebrafish exposed to 10 µM nitrite for 72 h showed a significant decrease compared with the control group (Figure 1, Panels D and E, respectively).

While there was no change in blood nitrite concentration (Figure 1F), a significant nitrite accumulation was observed in the muscle tissue of zebrafish exposed to 10 µM nitrite (Figure 1G).

3.2. Tissue Aerobic Capacity and Mitochondrial Dynamics

During state 2 respiration driven by a mixture of pyruvate and malate, a statistically significant reduction in oxygen consumption was observed in the mitochondria (Figure 2D) but not in the muscle homogenates (Figure 2A) of zebrafish exposed to nitrite.

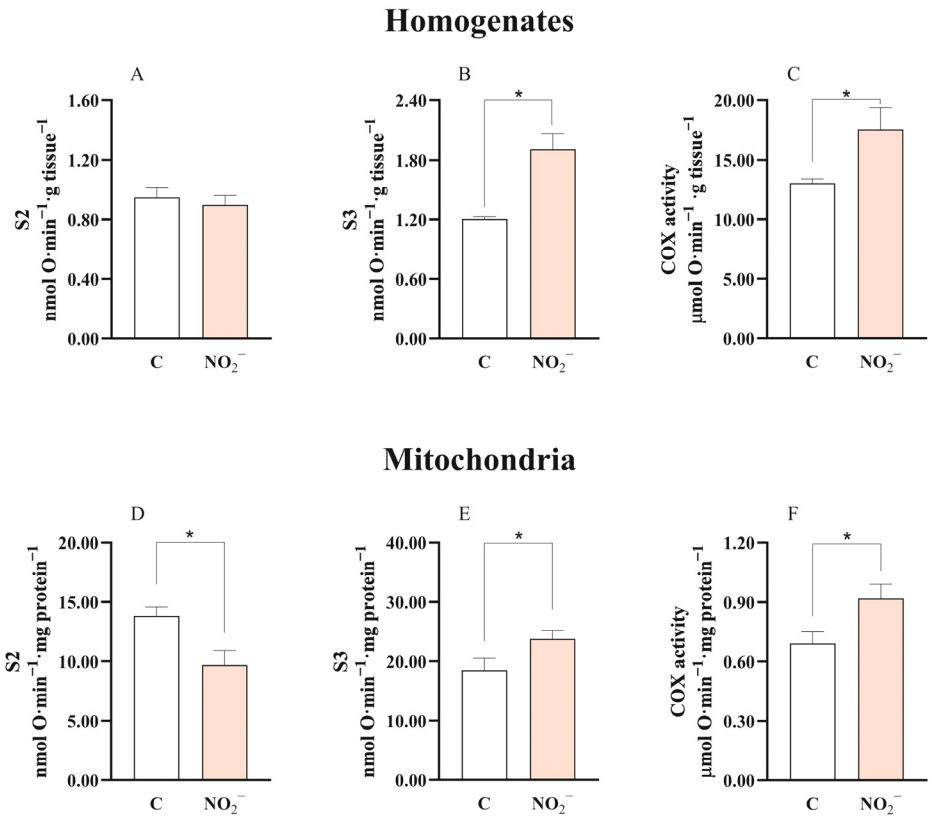

Figure 2. Oxygen consumption measured in the presence of pyruvate and malate, in the absence (state 2 of respiration, S2, (**A**,**D**)) and presence (state 3 of respiration, S3, (**B**,**E**)) of ADP, and COX activity (**C**,**F**) in homogenates (**A**–**C**) and mitochondria (**D**–**F**) from muscle tissue of control and 10 µM nitrite-exposed zebrafish. Data represent the mean ± SD of 3 replicated experiments. * $p < 0.05$.

In contrast, during state 3 respiration (Figure 2B,E), oxygen consumption increased in both muscle homogenates and isolated mitochondria from animals exposed to nitrite.

Finally, the maximum activity of COX, measured in samples treated with Lubrol, to facilitate enzyme activity detection, was significantly elevated by nitrite exposure in both muscle homogenates and mitochondria (Figures 2C and 2F, respectively).

The analysis of the activity of the electron transport chain (ETC) complexes in uncoupled mitochondria revealed a significant increase in all segments of ETC in zebrafish exposed to 10 µM nitrite (Figure 3). The activity between complexes I and IV, measured using NADH as the electron donor (Figure 3A), and that between complexes II and IV, assessed in the presence of rotenone (inhibitor of the electron flow between complexes I and III) and succinate (the electron donor) (Figure 3B), were doubled by the nitrite exposure. Furthermore, the complex IV activity measured with antimycin A (which blocks

electron flow at complex III) and TMPD plus ascorbate (which donates electrons directly to cytochrome c) (Figure 3C) was enhanced as well, confirming the COX activity increase detected in homogenates and isolated mitochondria (Figure 2F).

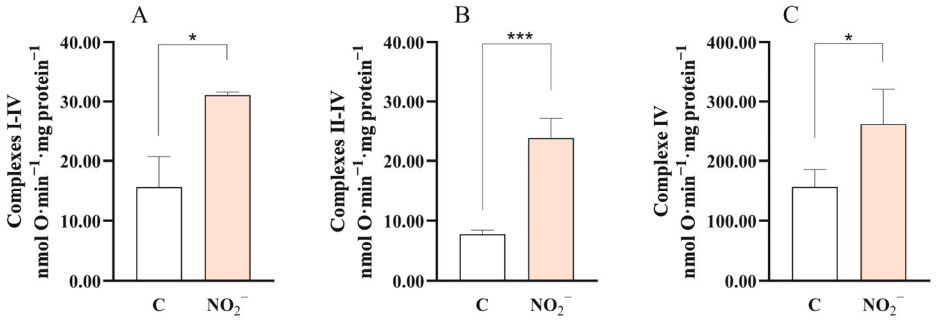

Figure 3. Activity of mitochondrial electron transport chain (ETC) in muscle isolated mitochondria of control and 10 µM nitrite-exposed zebrafish. (**A**): ETC activity between complexes I and IV; (**B**): ETC activity between complexes II and IV; (**C**): activity of complex IV. Data represent the mean ± SD of 3 replicated experiments. * $p < 0.05$; *** $p < 0.001$.

The mitochondrial population content, as evaluated by the cytochrome c levels (Figure 4A), was not significantly affected in the muscle of zebrafish exposed to nitrite. The no observed effect of nitrite on levels of dynamin and mitofusin demonstrates that fusion and fission were not affected after nitrite exposure (Figures 4B and 4C, respectively).

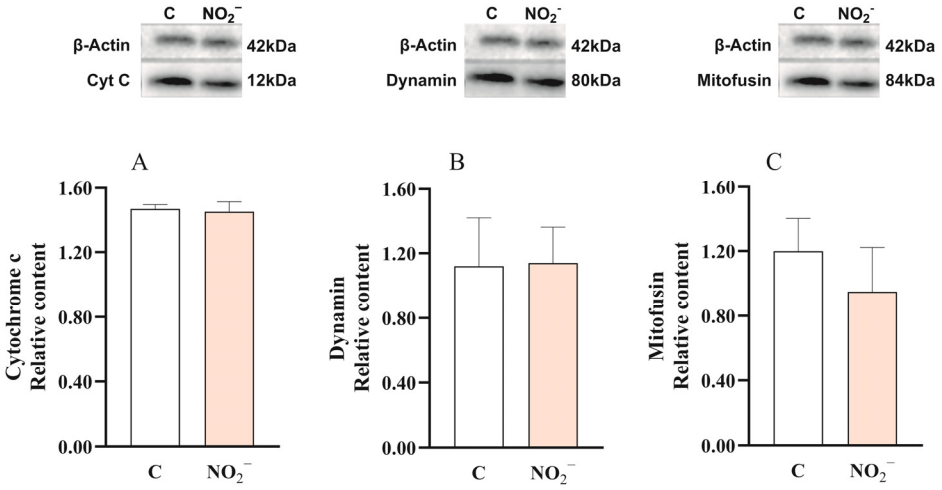

Figure 4. Western blot analysis of cytochrome c (**A**), dynamin (**B**), and mitofusin (**C**) levels in the muscle of control and 10 µM nitrite-exposed zebrafish. Data represent the mean ± SD of 3 replicated experiments.

3.3. Redox Homeostasis

Exposure of zebrafish to 10 µM nitrite for 72 h resulted in a significant increase in total reactive oxygen species (ROS) content in muscle tissue, as shown in Figure 5A. This increase in ROS was localized to extramitochondrial compartments, since mitochondrial total ROS content remained unchanged after nitrite exposure (Figure 5B).

The increased tissue ROS content corresponded with a significant rise in lipid hydroperoxide (Hp) levels (Figure 5C), indicating enhanced lipid peroxidation and oxidative damage to cell membranes. In contrast, treated animals showed higher total antioxidant capacity (TAC; Figure 5E) than the control group. This finding was further supported by a lower, though not statistically significant, resistance to oxidative stress (ΔHp, measured by changes in lipid hydroperoxide levels following prooxidant treatment; Figure 5D).

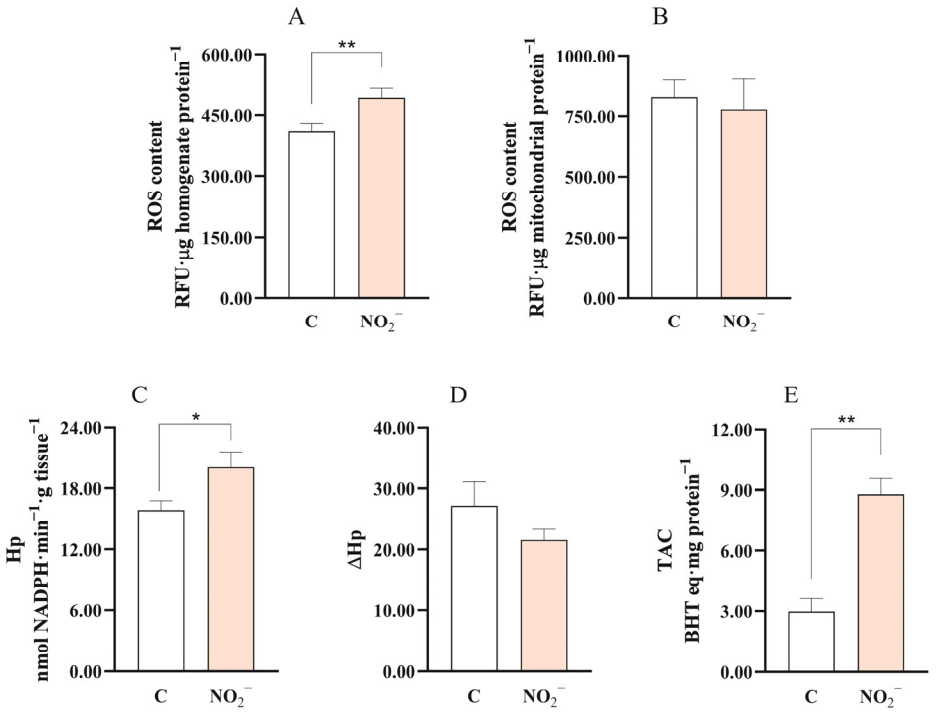

Figure 5. Redox homeostasis -linked parameters. Tissue (**A**) and mitochondrial (**B**) ROS content of control and 10µM nitrite-exposed zebrafish. Hydroperoxide levels (Hp, (**C**)), in vitro susceptibility to oxidants (ΔHp, (**D**)), and total antioxidant capacity (TAC, (**E**)) in muscle tissue homogenate of control and 10 µM nitrite-exposed zebrafish. Data represent the mean ± SD of 3 replicated experiments. * $p < 0.05$; ** $p < 0.01$.

3.4. Muscle Arginase Activity, and Urea and Lactate Content

The data reported in Figure 6 indicate that acute exposure to 10 µM nitrite also stimulated arginase activity and urea levels in the zebrafish (Figures 6A and 6B, respectively). Interestingly, lactate levels were also increased upon nitrite exposure (Figure 6C).

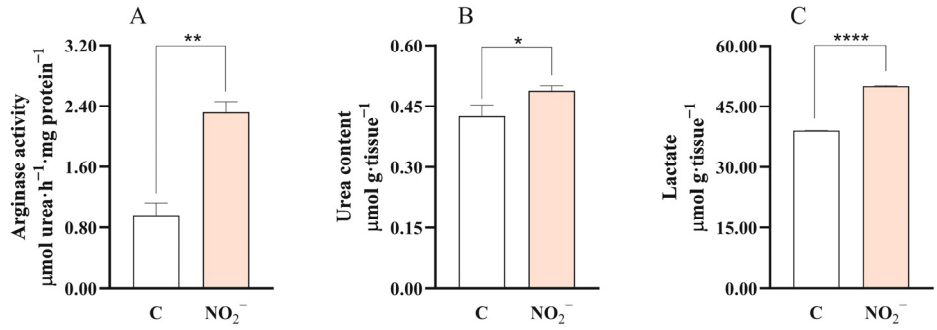

Figure 6. Arginase activity (**A**), urea (**B**), and lactate (**C**) content in the muscle of 10µM nitrite-exposed zebrafish. Data represent the mean ± SD of 3 replicated experiments. * $p < 0.05$; ** $p < 0.01$; **** $p < 0.0001$.

4. Discussion

This study shows that exposing adult zebrafish to a moderate, environmentally relevant concentration of nitrite (10 µM) [3] results in reduced routine metabolic rate (rMO_2) and decreased spontaneous activity. This exposure also increases blood HbNO levels, promotes nitrite accumulation in trunk muscle tissue, and modifies muscle aerobic capacity, associated with enhanced mitochondrial efficiency. In parallel, elevated antioxidant capacity, increased arginase activity, and higher muscle concentrations of urea and lactate were

observed. Overall, these findings indicate a disruption of nitric oxide (NO) homeostasis. A summary of results and their implications is reported in Figure 7.

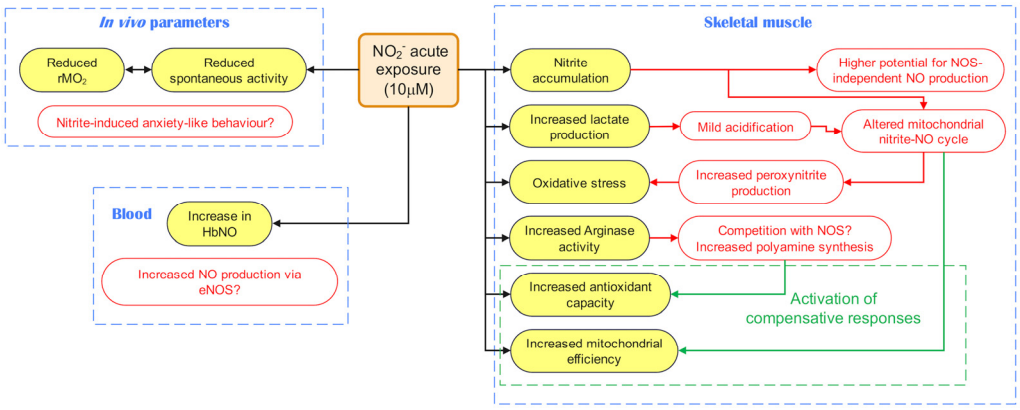

Figure 7. Summary of the primary effects (yellow boxes) induced by acute exposure to 10 μM NO_2^- in zebrafish, along with the proposed mechanisms or processes involved (red/green text).

It should be noted that the muscle samples analyzed in this study comprise both the trunk's white, fast-twitch fibers and red, slow-twitch fibers. Comparative data on nitrite homeostasis and metabolic capacities in these two muscle types in adult zebrafish are not currently available. Nevertheless, it is known that white muscle fibers, which support rapid anaerobic bursts, contain fewer and smaller mitochondria than red muscle, which is specialized for sustained oxidative swimming [63–65], and are less susceptible to oxidative damage under resting conditions [63]. In zebrafish, white muscle constitutes approximately 90% of the total trunk muscle, based on cross-sectional area [66]. Therefore, the results of this study likely primarily reflect disturbances in nitrite turnover within white muscle, which appears to be the main target of nitrite stress under moderate, sublethal exposure.

4.1. Effects on Hemoglobin

The blood's significant increase in HbNO (iron-nitrosyl hemoglobin) indicates an increase in NO production [44,45]. The corresponding 2% reduction in oxygen-carrying capacity is unlikely to induce significant tissue hypoxia in resting individuals [51], although it may become important during exercise. In mammals, the relation between HbNO levels and NO production is mainly due to an increased NO production by the vascular endothelial NOS (eNOS) [45]. NO from eNOS is a primary regulator of blood flow and pressure [67]. It is well known that in freshwater and seawater fish species, HbNO can form under conditions of nitrite stress. Nitrite reacts with deoxygenated Hb to form NO [68], which in turn can react with the ferrous heme forming HbNO. However, nitrite also reacts with oxygenated Hb to form metHb. Under nitrite stress in fish, metHb formation dominates over HbNO formation [31]. Since we find no change in metHb and nitrite blood levels, it is possible that the higher NO production results from increased synthesis by endothelial NOS. The slight reduction in the blood's total oxygen-carrying capacity levels might be responsible for the increased eNOS activity. It must be noted that eNOS expression in the fish vascular system is still debated [4]. Moreover, the relationship between oxygen-carrying capacity and eNOS activity is complex and highly context-dependent, involving several factors and regulatory feedback between red blood cells and the endothelium [69,70]. The putative eNOS stimulation in our experimental conditions is, at the moment, hypothetical but intriguing.

4.2. Effects on In Vivo Metabolism and Activity

In vivo, we observed a significant reduction in rMO_2 in animals exposed to 10 µM nitrite, likely associated with decreased spontaneous activity, as these parameters are closely related. Jensen [51] reported no change in routine oxygen consumption in zebrafish exposed for 48 h to 0.6 and 2 mM nitrite. The more extended exposure period in the present study (72 h) may have elicited a behavioral response to nitrite stress. Mild anxiety-like behavior, potentially reflected in reduced activity, has been documented in zebrafish following chronic exposure (2–4 weeks) to 0.4 mM nitrite [71]. It should be mentioned that both short-term [41] and long-term [72] exposure to high nitrite levels (in the mM range) have been shown to induce oxidative stress and morphological alterations in gill tissue, potentially reducing gill surface area. These changes can decrease oxygen uptake from water and lower metabolic activity. However, at the lower nitrite concentration used in this study, such a limiting effect on oxygen uptake is likely negligible.

4.3. Accumulation of Nitrite in Muscle Tissue

While nitrite in zebrafish blood is maintained unchanged, skeletal muscle significantly accumulates nitrite despite the higher environmental concentration, as shown in Figure 1F.

In mammals, muscle tissue can actively accumulate nitrite, possibly via sialin and chloride channels [73,74]. Muscle nitrite can be reduced to NO, contributing to local control of blood flow and muscle function [73,74]. The reduction of NO_2^- to bioactive NO occurs either through acidification or via several NO_2^- reductases. These include heme-globins such as myoglobin and cytoglobin, molybdenum-containing enzymes like xanthine oxidoreductase and aldehyde oxidase [10], as well as components of the mitochondrial electron transport chain, including the Q-cycle and cytochrome-c oxidase [6]. Fast-twitch muscles have a greater capacity for NO generation via nitrite reduction than slow-twitch muscles and the heart [75]. This property could be particularly significant for fast-twitch muscles during strenuous exercise or hypoxic conditions, as increased NO-mediated vasodilation could enhance muscle blood flow and delay fatigue.

Our results suggest a similar capacity for nitrite uptake in zebrafish muscle. Unlikely, there are no hints about the mechanism of uptake in fish, as there are very few studies on the active nitrite uptake capacity of fish skeletal muscle, which may vary by species. For example, muscle accumulation of nitrite has been reported in goldfish (*Carassius auratus*; [31]) but not in striped catfish (*Pangasianodon hypophthalmus*; [76]).

4.4. Nitrite Stimulates Arginase Activity

One factor that can affect NO homeostasis is the activity of arginase, a Mn-dependent enzyme that converts l-arginine to l-ornithine and urea. Arginase can compete with NOS for substrate [77] and can be stimulated under mechanical [78] or oxidative [79] stress. Arginase is stimulated by environmental nitrite stress (2 mM) in aquatic organisms [32]. Here, we confirm an increase in muscle arginase activity and a related rise in urea content, despite the lower environmental nitrite concentration. There are no clear hints on the mechanism of this nitrite-dependent stimulation. Fish possess both arginase-I (arg1, cytosolic, mainly in the liver, involved in the urea cycle) and arginase-II (arg2, mitochondrial, involved in non-ureogenic functions such as the synthesis of polyamines, bioactive molecules acting as antioxidants) [80,81]. In zebrafish, Arg2 is the predominant form of arginase, and its expression is strongly stimulated by acute hypoxia [82]. It should be noted that the urea cycle in zebrafish is active in young individuals, and rudimentary in adults [82]. So, it is possible that a nitrite-dependent oxidative stress stimulated Arg2 in muscle under our experimental conditions, favoring polyamine synthesis and contributing to antioxidant defenses. Another possibility is that increased arginase activity may reduce the arginine

supply to NOS (substrate competition), leading to enzyme uncoupling and reduced NO production, while generating superoxide from molecular oxygen [54]. However, despite fish possessing both nos1 and nos2 genes, there is, to date, no indication of their expression in white or red muscles [4].

4.5. Effects of Nitrite on Muscle NO Homeostasis, Redox State, and Mitochondrial Function

In mitochondria, nitrite can be reduced to NO by ETC, which in turn can be oxidized to NO_2^- by COX. Nitrite reduction is favored by acidosis (e.g., intense exercise, especially involving white muscles) or tissue hypoxia, while NO oxidation prevails under normoxia [5,83]. The nitrite-NO cycle may operate as a feedback system, adjusting mitochondrial activity to match oxygen availability and metabolic demand [5]. An increase in nitrite levels in the muscle cells might unbalance the cycle. Reducing COX-mediated NO oxidation would increase NO availability, favoring peroxynitrite formation and subsequent oxidative stress [84]. This process was likely favored by the mild acidification associated with the increased lactate levels in muscle tissue upon nitrite treatment, indicating stimulation of the glycolytic pathway. In mammals, fast-twitch muscle fibers have higher basal nitrite content. They are more prone to use nitrite as a substrate for nitric oxide (NO) production [75], especially under low-oxygen, low-pH conditions. Nitrite is known to stimulate glycolytic ATP synthesis in myocytes [85]. This hypothetical interpretation of the effects of increased nitrite content on muscle cells is supported by the higher total ROS levels in muscle tissue from treated animals and the corresponding increase in lipid peroxidation, as evidenced by elevated Hp levels. These results are in good agreement with previous studies showing that exposure to 15 mg/L of nitrite for 72 h induced a marked production of ROS, which caused oxidative damage in the liver tissue of the freshwater sea bream *Megalobrama amblycephala* [86].

Interestingly, these alterations in cellular NO homeostasis induced compensative responses in terms of mitochondrial efficiency and antioxidant defenses, as suggested by the increased total antioxidant capacity and decreased in vitro susceptibility to oxidants.

As a putative adaptive compensatory response to acute nitrite exposure, there was a significant increase in the potential rate of oxygen consumption during ADP-stimulated (State 3) respiration in both muscle homogenates and isolated mitochondria. In the tissue homogenate, the increase in ADP-stimulated respiration could also depend on increased mitochondrial population content, but the determination of the cytochrome c content excluded this possibility in muscle from nitrite-exposed zebrafish.

In both tissue homogenates and isolated mitochondria, oxygen consumption was measured under high oxygen availability, allowing us to focus on intrinsic respiratory capacity rather than oxygen limitation. Based on these observations, it can be proposed that mitochondrial activity is upregulated when nitrite is present. This adaptive compensatory mechanism would be particularly relevant in skeletal muscle, the most abundant tissue by body mass, which plays a predominant role in meeting the organism's overall metabolic demands [87]. The simultaneous reduction of rMO_2 and increased State 3 respiration provides strong evidence that nitrite treatment enhances the potential respiratory capacity of mitochondria.

Furthermore, mitochondrial ETC and COX activities, assessed in muscle homogenates and isolated mitochondria in the presence of Lubrol (which unmasks the enzyme's latent capacity), allowed us to detect their maximal activity. In zebrafish exposed to nitrite, a consistent increase in the activity of ETC segments spanning complexes I–IV and II–IV was observed, as well as a specific elevation in complex IV activity. Notably, the maximal activity of complex IV (COX) was also significantly enhanced. Together, these findings indicate that nitrite enhances the efficiency of ADP-driven respiration, promoting a broader

stimulation of the mitochondrial respiratory machinery and ultimately reinforcing its role in supporting cellular energy production under nitrite stress.

In zebrafish mitochondria exposed to nitrite, we observed a reduction in the rate of State 2 respiration. This process depends on maintaining the electrochemical proton gradient across the inner mitochondrial membrane [35]. Its decrease is consistent with the idea that nitrite exposure enhances mitochondrial efficiency by reducing oxygen consumption under non-phosphorylating conditions, thereby limiting energy loss through proton leakage. This effect strongly supports the notion that nitrite can fine-tune mitochondrial function to optimize energy utilization under stress conditions. Interestingly, these functional adjustments appear to occur without altering mitochondrial dynamics, as evidenced by the absence of significant changes in the relative abundance of key regulatory proteins, such as dynamin and mitofusin, following nitrite exposure. This observation suggests that the mitochondrial response to nitrite stress primarily involves mitochondrial bioenergetics rather than structural remodeling.

5. Conclusions

In conclusion, acute exposure to a moderate environmental concentration of nitrite induces nitrite accumulation in skeletal muscle and alters muscular metabolism and the redox state of adult zebrafish. Most of these effects can be interpreted as indices and consequences of an altered NO homeostasis in both the blood and muscle cells. The putative changes induced by nitrite accumulation in muscle cells, in the balance between NO synthesis and oxidation at the mitochondrial level, may alter the fine-tuning of mitochondrial function and cellular redox state, representing an intriguing mechanism of nitrite-induced environmental stress that deserves further detailed investigation.

Supplementary Materials: The following supporting information can be downloaded at: https://www.mdpi.com/article/10.3390/environments13010049/s1, experimental design, raw data and statistics for each figure.

Author Contributions: Conceptualization, C.A., G.N., P.V. and C.G.; Methodology, G.F., E.G., A.P. and M.T.M.T.; Software, C.A., G.N. and P.V.; Formal Analysis, G.N. and P.V.; Investigation, G.F., E.G., A.P. and M.T.M.T.; Data Curation, G.F., E.G., A.P. and M.T.M.T.; Writing—Original Draft Preparation, P.V., G.N. and C.A.; Writing—Review and Editing, P.V., G.N., C.A., G.F. and C.G. All authors have read and agreed to the published version of the manuscript.

Funding: This research received no external funding.

Institutional Review Board Statement: Animal care and experimental procedures were carried out in accordance with European Directive 2010/63/EU and Italian Law 26/2014 and were approved by the Committee for the Ethics of Animal Experiments at the University of Naples Federico II and the Italian Ministry of Health (Approval No. 767/2023-PR, 30 August 2023).

Data Availability Statement: All original data for this study are included in the Supplementary File, Figures S1–S6. Additional inquiries may be addressed to the corresponding authors.

Conflicts of Interest: The authors declare no conflicts of interest.

References

1. Philips, S.; Laanbroek, H.J.; Verstraete, W. Origin, Causes and Effects of Increased Nitrite Concentrations in Aquatic Environments. *Rev. Environ. Sci. Bio./Technol.* **2002**, *1*, 115–141. [CrossRef]
2. Yu, B.; Lyu, K.; Li, J.; Yang, Z.; Sun, Y. Combined Toxic Effects of Nitrite and Ammonia on Life History Traits of Daphnia Pulex. *Front. Environ. Sci.* **2022**, *10*, 1019483. [CrossRef]
3. Bian, D.-D.; Shi, Y.-X.; Zhang, X.; Liu, X.; Jiang, J.-J.; Zhu, X.-R.; Zhang, D.-Z.; Liu, Q.-N.; Zhu, B.-J.; Tang, B.-P. Nitrite Toxicity in Shrimp Aquaculture: Mechanisms, Health Impacts, and Sustainable Mitigation Strategies. *Rev. Aquac.* **2025**, *17*, e70062. [CrossRef]

4. Locascio, A.; Annona, G.; Caccavale, F.; D'Aniello, S.; Agnisola, C.; Palumbo, A. Nitric Oxide Function and Nitric Oxide Synthase Evolution in Aquatic Chordates. *Int. J. Mol. Sci.* **2023**, *24*, 11182. [CrossRef]
5. Shiva, S. Nitrite: A Physiological Store of Nitric Oxide and Modulator of Mitochondrial Function. *Redox Biol.* **2013**, *1*, 40–44. [CrossRef] [PubMed]
6. Kapil, V.; Khambata, R.S.; Jones, D.A.; Rathod, K.; Primus, C.; Massimo, G.; Fukuto, J.M.; Ahluwalia, A. The Noncanonical Pathway for In Vivo Nitric Oxide Generation: The Nitrate-Nitrite-Nitric Oxide Pathway. *Pharmacol. Rev.* **2020**, *72*, 692–766. [CrossRef] [PubMed]
7. Ghasemi, A. Quantitative Aspects of Nitric Oxide Production from Nitrate and Nitrite. *EXCLI J.* **2022**, *21*, 470–486. [CrossRef]
8. Piknova, B.; Park, J.W.; Tunau-Spencer, K.J.; Jenkins, A.; Hellinga, D.G.; Walter, P.J.; Cai, H.; Schechter, A.N. Skeletal Muscle, Skin, and Bone as Three Major Nitrate Reservoirs in Mammals: Chemiluminescence and 15N-Tracer Studies in Yorkshire Pigs. *Nutrients* **2024**, *16*, 2674. [CrossRef]
9. Piknova, B.; Park, J.W.; Schechter, A.N. Nitrate as Warden of Nitric Oxide Homeostasis in Mammals. *Nutrients* **2025**, *17*, 1544. [CrossRef]
10. Bryan, N.S.; Fernandez, B.O.; Bauer, S.M.; Garcia-Saura, M.F.; Milsom, A.B.; Rassaf, T.; Maloney, R.E.; Bharti, A.; Rodriguez, J.; Feelisch, M. Nitrite Is a Signaling Molecule and Regulator of Gene Expression in Mammalian Tissues. *Nat. Chem. Biol.* **2005**, *1*, 290–297. [CrossRef]
11. Pellegrino, D.; Parisella, M.L. Nitrite as a Physiological Source of Nitric Oxide and a Signalling Molecule in the Regulation of the Cardiovascular System in Both Mammalian and Non-Mammalian Vertebrates. *Recent Pat. Cardiovasc. Drug Discov.* **2010**, *5*, 91–96. [CrossRef] [PubMed]
12. DeMartino, A.W.; Kim-Shapiro, D.B.; Patel, R.P.; Gladwin, M.T. Nitrite and Nitrate Chemical Biology and Signalling. *Br. J. Pharmacol.* **2019**, *176*, 228–245. [CrossRef]
13. Diaz, R.J. Overview of Hypoxia around the World. *J. Environ. Qual.* **2001**, *30*, 275. [CrossRef]
14. Steckbauer, A.; Duarte, C.M.; Carstensen, J.; Vaquer-Sunyer, R.; Conley, D.J. Ecosystem Impacts of Hypoxia: Thresholds of Hypoxia and Pathways to Recovery. *Environ. Res. Lett.* **2011**, *6*, 025003. [CrossRef]
15. Fusi, M.; Stephenson, F.; Navarrete, S.A.; Tapia, F.J.; Largier, J.L.; Marasco, R.; Rueger, T.; MacDonald, C.; Daffonchio, D.; Fernandez, M.; et al. The Ecology of the Oxyscape in Coastal Ecosystems. *Trends Ecol. Evol.* **2025**, *40*, 791–804. [CrossRef]
16. Jensen, F.B. The Role of Nitrite in Nitric Oxide Homeostasis: A Comparative Perspective. *Biochim. Biophys. Acta (BBA) Bioenerg.* **2009**, *1787*, 841–848. [CrossRef]
17. Pedersen, C.L.; Faggiano, S.; Helbo, S.; Gesser, H.; Fago, A. Roles of Nitric Oxide, Nitrite and Myoglobin on Myocardial Efficiency in Trout (*Oncorhynchus mykiss*) and Goldfish (*Carassius auratus*): Implications for Hypoxia Tolerance. *J. Exp. Biol.* **2010**, *213*, 2755–2762. [CrossRef]
18. Corti, P.; Xue, J.; Tejero, J.; Wajih, N.; Sun, M.; Stolz, D.B.; Tsang, M.; Kim-Shapiro, D.B.; Gladwin, M.T. Globin X Is a Six-Coordinate Globin That Reduces Nitrite to Nitric Oxide in Fish Red Blood Cells. *Proc. Natl. Acad. Sci. USA* **2016**, *113*, 8538–8543. [CrossRef]
19. Fago, A.; Jensen, F.B. Hypoxia Tolerance, Nitric Oxide, and Nitrite: Lessons From Extreme Animals. *Physiology* **2015**, *30*, 116–126. [CrossRef] [PubMed]
20. Filice, M.; Imbrogno, S.; Gattuso, A.; Cerra, M.C. Hypoxic and Thermal Stress: Many Ways Leading to the NOS/NO System in the Fish Heart. *Antioxidants* **2021**, *10*, 1401. [CrossRef]
21. Hansen, M.N.; Gerber, L.; Jensen, F.B. Nitric Oxide Availability in Deeply Hypoxic Crucian Carp: Acute and Chronic Changes and Utilization of Ambient Nitrite Reservoirs. *Am. J. Physiol. Regul. Integr. Comp. Physiol.* **2016**, *310*, R532–R540. [CrossRef]
22. Lewis, W.M., Jr.; Morris, D.P. Toxicity of Nitrite to Fish: A Review. *Trans. Am. Fish. Soc.* **1986**, *115*, 183–195. [CrossRef]
23. Jensen, F.B. Nitrite Disrupts Multiple Physiological Functions in Aquatic Animals. *Comp. Biochem. Physiol. Part A Mol. Integr. Physiol.* **2003**, *135*, 9–24. [CrossRef]
24. Kroupová, H.K.; Valentová, O.; Svobodová, Z.; Šauer, P.; Máchová, J. Toxic Effects of Nitrite on Freshwater Organisms: A Review. *Rev. Aquac.* **2018**, *10*, 525–542. [CrossRef]
25. Martinez, M.A.; Mancha, F.; Gomes, A.; Huertas, M. Toxicokinetic of Sublethal Concentrations of Nitrite in Goldfish (*Carassius auratus*). *FASEB J.* **2020**, *34*, 1. [CrossRef]
26. Margiocco, C.; Arillo, A.; Mensi, P.; Schenone, G. Nitrite Bioaccumulation in Salmo Gairdneri Rich. and Hematological Consequences. *Aquat. Toxicol.* **1983**, *3*, 261–270. [CrossRef]
27. García-Robledo, E.; Corzo, A.; Papaspyrou, S. A Fast and Direct Spectrophotometric Method for the Sequential Determination of Nitrate and Nitrite at Low Concentrations in Small Volumes. *Mar. Chem.* **2014**, *162*, 30–36. [CrossRef]
28. Zhang, F.; Zhu, X.; Jiao, Z.; Liu, X.; Zhang, H. Sensitive Naked Eye Detection and Quantification Assay for Nitrite by a Fluorescence Probe in Various Water Resources. *Spectrochim. Acta Part A Mol. Biomol. Spectrosc.* **2018**, *200*, 275–280. [CrossRef]
29. Mai, Y.; Debruille, K.; Mikhail, I.; Gupta, V.; Murray, E.; Frantsuzov, R.; Paull, B. Measuring Nitrite and Nitrate in Rain and River Water Samples Using a Portable Ion Chromatograph in Step-Gradient Mode and High Sensitivity Detection Flow Cell. *J. Sep. Sci.* **2025**, *48*, e70134. [CrossRef]

30. Liu, G.; Verdegem, M.; Ye, Z.; Zhao, J.; Xiao, J.; Liu, X.; Liang, Q.; Xiang, K.; Zhu, S. Advancing Aquaculture Sustainability: A Comprehensive Review of Biofloc Technology Trends, Innovative Research Approaches, and Future Prospects. *Rev. Aquac.* **2025**, *17*, e12970. [CrossRef]
31. Jensen, F.B.; Hansen, M.N. Differential Uptake and Metabolism of Nitrite in Normoxic and Hypoxic Goldfish. *Aquat. Toxicol.* **2011**, *101*, 318–325. [CrossRef]
32. Napolitano, G.; Fasciolo, G.; Agnisola, C.; Venditti, P. Urea Excretion and Arginase Activity as New Biomarkers for Nitrite Stress in Freshwater Aquatic Animals. *Water* **2021**, *13*, 3521. [CrossRef]
33. Tengan, C.H.; Rodrigues, G.S.; Godinho, R.O. Nitric Oxide in Skeletal Muscle: Role on Mitochondrial Biogenesis and Function. *Int. J. Mol. Sci.* **2012**, *13*, 17160–17184. [CrossRef]
34. Poderoso, J.J.; Helfenberger, K.; Poderoso, C. The Effect of Nitric Oxide on Mitochondrial Respiration. *Nitric Oxide* **2019**, *88*, 61–72. [CrossRef] [PubMed]
35. Napolitano, G.; Fasciolo, G.; Venditti, P. Mitochondrial Management of Reactive Oxygen Species. *Antioxidants* **2021**, *10*, 1824. [CrossRef]
36. Benamar, A.; Rolletschek, H.; Borisjuk, L.; Avelange-Macherel, M.-H.; Curien, G.; Mostefai, H.A.; Andriantsitohaina, R.; Macherel, D. Nitrite–Nitric Oxide Control of Mitochondrial Respiration at the Frontier of Anoxia. *Biochim. Biophys. Acta (BBA) Bioenerg.* **2008**, *1777*, 1268–1275. [CrossRef]
37. Piacenza, L.; Zeida, A.; Trujillo, M.; Radi, R. The Superoxide Radical Switch in the Biology of Nitric Oxide and Peroxynitrite. *Physiol. Rev.* **2022**, *102*, 1881–1906. [CrossRef] [PubMed]
38. Jia, R.; Han, C.; Lei, J.-L.; Liu, B.-L.; Huang, B.; Huo, H.-H.; Yin, S.-T. Effects of Nitrite Exposure on Haematological Parameters, Oxidative Stress and Apoptosis in Juvenile Turbot (*Scophthalmus maximus*). *Aquat. Toxicol.* **2015**, *169*, 1–9. [CrossRef]
39. Gao, X.-Q.; Fei, F.; Huo, H.H.; Huang, B.; Meng, X.S.; Zhang, T.; Liu, B.-L. Effect of Acute Exposure to Nitrite on Physiological Parameters, Oxidative Stress, and Apoptosis in Takifugu Rubripes. *Ecotoxicol. Environ. Saf.* **2020**, *188*, 109878. [CrossRef] [PubMed]
40. de Sousa Miranda, D.H.; Maltez, L.C.; Campello, M.E.S.; Córdova, J.F.L.; Rodrigues, R.V.; Sampaio, L.A.; Okamoto, M.H. Acute Toxicity and Sublethal Effects of Nitrite on Oxidative Stress in Early Juvenile Brazilian Flounder, *Paralichthys orbignyanus*. *Aquac. Res.* **2022**, *53*, 1939–1946. [CrossRef]
41. Xu, Z.; Zhang, H.; Guo, M.; Fang, D.; Mei, J.; Xie, J. Analysis of Acute Nitrite Exposure on Physiological Stress Response, Oxidative Stress, Gill Tissue Morphology and Immune Response of Large Yellow Croaker (*Larimichthys crocea*). *Animals* **2022**, *12*, 1791. [CrossRef]
42. Kim, J.-H.; Kang, Y.J.; Lee, K.M. Effects of Nitrite Exposure on the Hematological Properties, Antioxidant and Stress Responses of Juvenile Hybrid Groupers, *Epinephelus lanceolatus* ♂× *Epinephelus fuscoguttatus* ♀. *Antioxidants* **2022**, *11*, 545. [CrossRef]
43. Bourdineaud, J.-P.; Rossignol, R.; Brèthes, D. Zebrafish: A Model Animal for Analyzing the Impact of Environmental Pollutants on Muscle and Brain Mitochondrial Bioenergetics. *Int. J. Biochem. Cell Biol.* **2013**, *45*, 16–22. [CrossRef] [PubMed]
44. Gladwin, M.T.; Schechter, A.N.; Kim-Shapiro, D.B.; Patel, R.P.; Hogg, N.; Shiva, S.; Cannon, R.O.; Kelm, M.; Wink, D.A.; Espey, M.G.; et al. The Emerging Biology of the Nitrite Anion. *Nat. Chem. Biol.* **2005**, *1*, 308–314. [CrossRef]
45. Zotti, F.D.; Lobysheva, I.I.; Balligand, J.-L. Nitrosyl-Hemoglobin Formation in Rodent and Human Venous Erythrocytes Reflects NO Formation from the Vasculature in Vivo. *PLoS ONE* **2018**, *13*, e0200352. [CrossRef]
46. Belcher, R.; Rodriguez-Vazquez, J.A.; Stephen, W.I. A Sensitive Method for the Ultraviolet Spectrophotometric Determination of Chloride. *Anal. Chim. Acta* **1972**, *61*, 223–232. [CrossRef]
47. Shechter, H.; Gruener, N.; Shuval, H.I. A Micromethod for the Determination of Nitrite in Blood. *Anal. Chim. Acta* **1972**, *60*, 93–99. [CrossRef]
48. European Commission. *Directorate General for Health and Food Safety. Revision of Annexes III and IV of Directive 2010/63/EU on the Protection of Animals Used for Scientific Purposes Regarding Accommodation Parameters and Methods of Killing for Zebrafish, and Accommodation Parameters for Passerine Birds*; Publications Office of the European Union: Luxembourg, 2024.
49. Uliano, E.; Cataldi, M.; Carella, F.; Migliaccio, O.; Iaccarino, D.; Agnisola, C. Effects of Acute Changes in Salinity and Temperature on Routine Metabolism and Nitrogen Excretion in Gambusia (*Gambusia affinis*) and Zebrafish (*Danio rerio*). *Comp. Biochem. Physiol. Part A Mol. Integr. Physiol.* **2010**, *157*, 283–290. [CrossRef]
50. Agnisola, C.; Femiano, S. Studies on Routine Metabolism in Adult Zebrafish, *Danio rerio*. *Acta Physiol.* **2006**, *187*, 49.
51. Jensen, F.B. Nitric Oxide Formation from Nitrite in Zebrafish. *J. Exp. Biol.* **2007**, *210*, 3387–3394. [CrossRef]
52. Dunn, J.F.; Hochachka, P.W. Metabolic Responses of Trout (*Salmo gairdneri*) to Acute Environmental Hypoxia. *J. Exp. Biol.* **1986**, *123*, 229–242. [CrossRef]
53. Rahmatullah, M.; Boyde, T.R.C. Improvements in the Determination of Urea Using Diacetyl Monoxime; Methods with and without Deproteinisation. *Clin. Chim. Acta* **1980**, *107*, 3–9. [CrossRef]
54. Romero, M.J.; Platt, D.H.; Tawfik, H.E.; Labazi, M.; El-Remessy, A.B.; Bartoli, M.; Caldwell, R.B.; Caldwell, R.W. Diabetes-Induced Coronary Vascular Dysfunction Involves Increased Arginase Activity. *Circ. Res.* **2008**, *102*, 95–102. [CrossRef]

55. Rees, B.B.; Boily, P.; Williamson, A.C. Exercise- and Hypoxia-Induced Anaerobic Metabolism and Recovery: A Student Laboratory Exercise Using Teleost Fish. *Adv. Physiol. Edu.* **2009**, *33*, 72–77. [CrossRef]
56. Villani, G.; Greco, M.; Papa, S.; Attardi, G. Low Reserve of Cytochrome *c* Oxidase Capacity in Vivo in the Respiratory Chain of a Variety of Human Cell Types. *J. Biol. Chem.* **1998**, *273*, 31829–31836. [CrossRef] [PubMed]
57. Napolitano, G.; Fasciolo, G.; Magnacca, N.; Goglia, F.; Lombardi, A.; Venditti, P. Oxidative Damage and Mitochondrial Functionality in Hearts from KO UCP3 Mice Housed at Thermoneutrality. *J. Physiol. Biochem.* **2022**, *78*, 415–425. [CrossRef]
58. Acin-Perez, R.; Benador, I.Y.; Petcherski, A.; Veliova, M.; Benavides, G.A.; Lagarrigue, S.; Caudal, A.; Vergnes, L.; Murphy, A.N.; Karamanlidis, G.; et al. A Novel Approach to Measure Mitochondrial Respiration in Frozen Biological Samples. *EMBO J.* **2020**, *39*, e104073. [CrossRef] [PubMed]
59. Napolitano, G.; Fasciolo, G.; Muscari Tomajoli, M.T.; Venditti, P. Changes in the Mitochondria in the Aging Process—Can α-Tocopherol Affect Them? *Int. J. Mol. Sci.* **2023**, *24*, 12453. [CrossRef]
60. Fasciolo, G.; Napolitano, G.; Aprile, M.; Cataldi, S.; Costa, V.; Ciccodicola, A.; Di Meo, S.; Venditti, P. Hepatic Insulin Resistance in Hyperthyroid Rat Liver: Vitamin E Supplementation Highlights a Possible Role of ROS. *Antioxidants* **2022**, *11*, 1295. [CrossRef] [PubMed]
61. Heath, R.L.; Tappel, A.L. A New Sensitive Assay for the Measurement of Hydroperoxides. *Anal. Biochem.* **1976**, *76*, 184–191. [CrossRef]
62. La Pietra, A.; Fasciolo, G.; Lucariello, D.; Motta, C.M.; Venditti, P.; Ferrandino, I. Polystyrene Microplastics Effects on Zebrafish Embryological Development: Comparison of Two Different Sizes. *Environ. Toxicol. Pharmacol.* **2024**, *106*, 104371. [CrossRef]
63. Neurohr, J.M.; Paulson, E.T.; Kinsey, S.T. A Higher Mitochondrial Content Is Associated with Greater Oxidative Damage, Oxidative Defenses, Protein Synthesis and ATP Turnover in Resting Skeletal Muscle. *J. Exp. Biol.* **2021**, *224*, jeb242462. [CrossRef]
64. Rostad, K.O.; Trognitz, T.; Frøyset, A.K.; Bifulco, E.; Fladmark, K.E. Accelerated Sarcopenia Phenotype in the DJ-1/Park7-Knockout Zebrafish. *Antioxidants* **2024**, *13*, 1509. [CrossRef]
65. Lu, Z.; Li, Q.; Yongo, E.; Xiao, J.; Guo, Z. Comparative Energy Metabolism in Red and White Muscles of Juvenile Yellowfin Tuna, *Thunnus albacore*. *Front. Mar. Sci.* **2025**, *12*, 1585044. [CrossRef]
66. Hasumura, T.; Meguro, S. Exercise Quantity-Dependent Muscle Hypertrophy in Adult Zebrafish (*Danio rerio*). *J. Comp. Physiol. B* **2016**, *186*, 603–614. [CrossRef] [PubMed]
67. Tran, N.; Garcia, T.; Aniqa, M.; Ali, S.; Ally, A.; Nauli, S.M. Endothelial Nitric Oxide Synthase (eNOS) and the Cardiovascular System: In Physiology and in Disease States. *Am. J. Biomed. Sci. Res.* **2022**, *15*, 155.
68. Kim-Shapiro, D.B.; Gladwin, M.T.; Patel, R.P.; Hogg, N. The Reaction between Nitrite and Hemoglobin: The Role of Nitrite in Hemoglobin-Mediated Hypoxic Vasodilation. *J. Inorg. Biochem.* **2005**, *99*, 237–246. [CrossRef]
69. Beleslin-Cokic, B.B.; Cokic, V.P.; Yu, X.; Weksler, B.B.; Schechter, A.N.; Noguchi, C.T. Erythropoietin and Hypoxia Stimulate Erythropoietin Receptor and Nitric Oxide Production by Endothelial Cells. *Blood* **2004**, *104*, 2073–2080. [CrossRef]
70. Leo, F.; Suvorava, T.; Heuser, S.K.; Li, J.; LoBue, A.; Barbarino, F.; Piragine, E.; Schneckmann, R.; Hutzler, B.; Good, M.E.; et al. Red Blood Cell and Endothelial eNOS Independently Regulate Circulating Nitric Oxide Metabolites and Blood Pressure. *Circulation* **2021**, *144*, 870–889. [CrossRef]
71. García-Jaramillo, M.; Beaver, L.M.; Truong, L.; Axton, E.R.; Keller, R.M.; Prater, M.C.; Magnusson, K.R.; Tanguay, R.L.; Stevens, J.F.; Hord, N.G. Nitrate and Nitrite Exposure Leads to Mild Anxiogenic-like Behavior and Alters Brain Metabolomic Profile in Zebrafish. *PLoS ONE* **2020**, *15*, e0240070. [CrossRef]
72. Wang, X.; Tang, Y.; Yang, H.; He, Y.; Ou-Yang, K.; Wang, L.; Zhang, Q.; Li, D.; Li, L. Increased CO_2 Concentration Mitigates the Impact of Nitrite on Zebrafish (*Danio rerio*) Liver and Gills. *Fishes* **2025**, *10*, 205. [CrossRef]
73. Wylie, L.J.; Park, J.W.; Vanhatalo, A.; Kadach, S.; Black, M.I.; Stoyanov, Z.; Schechter, A.N.; Jones, A.M.; Piknova, B. Human Skeletal Muscle Nitrate Store: Influence of Dietary Nitrate Supplementation and Exercise. *J. Physiol.* **2019**, *597*, 5565–5576. [CrossRef]
74. Srihirun, S.; Park, J.W.; Teng, R.; Sawaengdee, W.; Piknova, B.; Schechter, A.N. Nitrate Uptake and Metabolism in Human Skeletal Muscle Cell Cultures. *Nitric Oxide* **2020**, *94*, 1–8. [CrossRef] [PubMed]
75. Majerczak, J.; Kij, A.; Drzymala-Celichowska, H.; Kus, K.; Karasinski, J.; Nieckarz, Z.; Grandys, M.; Celichowski, J.; Szkutnik, Z.; Hendgen-Cotta, U.B.; et al. Nitrite Concentration in the Striated Muscles Is Reversely Related to Myoglobin and Mitochondrial Proteins Content in Rats. *Int. J. Mol. Sci.* **2022**, *23*, 2686. [CrossRef]
76. Ha, N.T.K.; Huong, D.T.T.; Phuong, N.T.; Bayley, M.; Jensen, F.B. Impact and Tissue Metabolism of Nitrite at Two Acclimation Temperatures in Striped Catfish (*Pangasianodon hypophthalmus*). *Aquat. Toxicol.* **2019**, *212*, 154–161. [CrossRef]
77. Rath, M.; Müller, I.; Kropf, P.; Closs, E.I.; Munder, M. Metabolism via Arginase or Nitric Oxide Synthase: Two Competing Arginine Pathways in Macrophages. *Front. Immunol.* **2014**, *5*, 532. [CrossRef]
78. Thacher, T.N.; Gambillara, V.; Riche, F.; Silacci, P.; Stergiopulos, N.; da Silva, R.F. Regulation of Arginase Pathway in Response to Wall Shear Stress. *Atherosclerosis* **2010**, *210*, 63–70. [CrossRef] [PubMed]

79. Iyamu, E.W.; Perdew, H.; Woods, G.M. Cysteine–Iron Promotes Arginase Activity by Driving the Fenton Reaction. *Biochem. Biophys. Res. Commun.* **2008**, *376*, 116–120. [CrossRef] [PubMed]
80. Benedicenti, O.; Wang, T.; Wangkahart, E.; Milne, D.J.; Holland, J.W.; Collins, C.; Secombes, C.J. Characterisation of Arginase Paralogues in Salmonids and Their Modulation by Immune Stimulation/Infection. *Fish Shellfish. Immunol.* **2017**, *61*, 138–151. [CrossRef]
81. Banerjee, B.; Khrystoforova, I.; Polis, B.; Zvi, I.B.; Karasik, D. Acute Hypoxia Elevates Arginase 2 and Induces Polyamine Stress Response in Zebrafish via Evolutionarily Conserved Mechanism. *Cell. Mol. Life Sci.* **2021**, *79*, 41. [CrossRef]
82. Braun, M.H.; Steele, S.L.; Ekker, M.; Perry, S.F. Nitrogen Excretion in Developing Zebrafish (*Danio rerio*): A Role for Rh Proteins and Urea Transporters. *Am. J. Physiol. Ren. Physiol.* **2009**, *296*, F994–F1005. [CrossRef]
83. Basu, S.; Azarova, N.A.; Font, M.D.; King, S.B.; Hogg, N.; Gladwin, M.T.; Shiva, S.; Kim-Shapiro, D.B. Nitrite Reductase Activity of Cytochrome C. *J. Biol. Chem.* **2008**, *283*, 32590–32597. [CrossRef] [PubMed]
84. Pearson, T.; McArdle, A.; Jackson, M.J. Nitric Oxide Availability Is Increased in Contracting Skeletal Muscle from Aged Mice, but Does Not Differentially Decrease Muscle Superoxide. *Free Radic. Biol. Med.* **2015**, *78*, 82–88. [CrossRef] [PubMed]
85. Wynne, A.G.; Affourtit, C. Nitrite Lowers the Oxygen Cost of ATP Supply in Cultured Skeletal Muscle Cells by Stimulating the Rate of Glycolytic ATP Synthesis. *PLoS ONE* **2022**, *17*, e0266905. [CrossRef]
86. Sun, S.; Ge, X.; Zhu, J.; Xuan, F.; Jiang, X. Identification and mRNA Expression of Antioxidant Enzyme Genes Associated with the Oxidative Stress Response in the Wuchang Bream (*Megalobrama amblycephala* Yih) in Response to Acute Nitrite Exposure. *Comp. Biochem. Physiol. Part C Toxicol. Pharmacol.* **2014**, *159*, 69–77. [CrossRef]
87. Sartori, R.; Romanello, V.; Sandri, M. Mechanisms of Muscle Atrophy and Hypertrophy: Implications in Health and Disease. *Nat. Commun.* **2021**, *12*, 330. [CrossRef]